IEEE Access
Multidisciplinary | Rapid Review | Open Access Journal

Received December 10, 2018, accepted December 17, 2018, date of publication January 8, 2019, date of current version January 23, 2019.

Digital Object Identifier 10.1109/ACCESS.2018.2889333

A 1-D Tightly Coupled Dipole Array for Broadband mmWave Communication

JAE-YEON SHIM, JONG-GYU GO, AND JAE-YOUNG CHUNG, (Senior Member, IEEE)
Department of Electrical and Information Engineering, Seoul National University of Science and Technology, Seoul 01811, South Korea

Corresponding author: Jae-Young Chung (jychung@seoultech.ac.kr)

This work was supported by the Advanced Research Project funded by the Seoul National University of Science and Technology (Seoultech).

ABSTRACT A wideband phased array antenna for the use in 5G millimeter-wave (mmWave) mobile terminal is presented. The proposed array antenna was designed based on the tightly coupled dipole array (TCDA) technique to achieve a low profile and broadband impedance matching characteristic. Unlike the previously reported TCDAs implemented with 2D arrays on a vertical ground plane, the proposed 1D array antenna exhibited the maximum beam direction parallel to the ground, which is suitable for mobile terminal applications. Using a full-wave electromagnetic simulation tool, a 1×8 TCDA was designed on a multilayer substrate including a reflector surface in the middle to replace a vertical ground plane. Prototypes were fabricated and measured with feeding networks designed for 0° and 30° scanning scenarios. The size of the proposed antenna (excluding the feeding network) was $42.3 \times 12.05 \times 0.535$ mm^3. The measured bandwidth that subjects to $S_{11} < -10$ dB criterion was 22.5–32.5 GHz, which covers most of the worldwide 5G mmWave frequency band candidates at the 20-GHz band range.

INDEX TERMS 5G mobile communication, antenna arrays, mobile terminal, millimeter-wave (mmWave), phased array, wideband.

I. INTRODUCTION

Communication providers and mobile terminal manufacturers are putting great effort into commercializing the fifth-generation (5G) mobile communication system to provide enhanced mobile broadband communication services using a 10 times wider bandwidth that the current 4G system [1]. To meet the demand, the use of millimeter-wave (mmWave) bands above 20 GHz have been proposed to secure a wide bandwidth [2]. At the World Radiocommunication Conference-15 (WRC-15) in 2015, several mmWave frequency bands were discussed as the 5G wireless communication candidates and it is supposed to be selected at WRC-19 in 2019 [3], [4]. Table 1 shows candidate bands in the 20 – 30 GHz range.

Previously, mmWave frequency bands have been used for military, satellite, and high-capacity point-to-point communications. They are mainly for fixed wireless links or inter-facility communications rather than mobile communications and the designated frequency bands vary from country to country. Therefore, it will not be easy to select a single standard 5G mmWave frequency band which is agreed upon all countries [3]. In this context, the development of wideband RF components and antennas that can cover worldwide mmWave band candidates is called for.

Due to the high transmission loss of mmWave, it is required to use a phased array antenna with high directivity and adaptive beam scanning capability both in the base station and mobile terminal. Compared to copious amount of array antenna designs proposed for a 5G mmWave base station [5]–[9], a relatively small number of studies exist for a mobile terminal. For the latter, the array should be low profile and have a small footprint to fit in the shallow and limited area in a mobile terminal while maintaining a low reflection coefficient (S_{11}) and high antenna gain in various scanning angles. Several proof-of-concept designs have been reported [10]–[13], but their bandwidths were limited to less than 3 GHz with a center. Wideband arrays were presented in [14] and [15], but they did not cover relatively low-frequency bands below 26 GHz [14] and not support end-fire radiation parallel to the antenna substrate [15].

One design technique to improve array antenna bandwidth is the Tightly Coupled Dipole Array (TCDA) first proposed by Munk [16]. TCDA utilizes intentional mutual coupling between neighboring elements to offset the inductance that

TABLE 1. 5G candidate frequency bands around 20 GHz.

Union & Countries	5G Candidate Bands [GHz]
ITU	24.25 – 27.5
Europe	24.25 – 27.5
USA	27.5 – 28.35
South Korea	26.5 – 29.5
China	24.75 – 27.5
Japan	27.5 – 29.5

occurs near the ground plane. Moreover, by tight capacitive coupling between the adjacent elements, the array can support the currents at wavelengths much larger than the dimensions of a single elements, thereby enabling wideband and low profile implementation [16]. Various TCDA designs have been reported with outstanding performances; for example, bandwidth improvements with an integrated double balanced-to-unbalanced (balun) structure and superstrate [17], [18] and wide-scanning angle in both the azimuth and elevation angles [19]. More recently, 1D TCDAs with only the azimuth scanning capability have been reported for narrow space implementation [20], [21].

However, all of the above are vertically implemented over a ground plane to achieve a broadside radiation pattern, and often require a superstrate [20] or vertical walls [21] to maintain performance, which is not suitable for the application in mobile terminals. Therefore, for a TCDA to operate in mobile terminal, the array should exhibit the maximum beam direction parallel to the ground. In addition, it should be capable of fabrication using a printed-circuit-board (PCB) technology.

In this paper, we propose a 1D TCDA mmWave antenna design for mobile terminal applications, which provides almost 10 GHz impedance matching bandwidth at the 20 GHz band. The designed 1×8 TCDA has a footprint of $42.3 \times 12.05 \times 0.535$ mm^3 which is compact enough to install in the edge of mobile terminals. To demonstrate the performance, the 1×8 TCDA antenna with feeding network was designed, fabricated and measured.

II. ANTENNA DESIGN

A. GEOMETRY OF THE PROPOSED TCDA

Fig. 1 depicts the y-z and x-y planes of the proposed three-layer TCDA antenna schematic. Layers 1 and 3 consist of dipole arrays and an excitation baluns, respectively. In Layer 2, a reflector is placed to compensate for radiation characteristic degradation due to the absent of the vertical ground plane. The proposed TCDA antenna has eight unit cells arranged at intervals of balun $D_{feed} = 4.8$ mm, and the overall size of the antenna is $W_{sub} = 42.3$ mm and $H_{sub} = 12.05$ mm. The substrate used was Taconic RF-35 laminate with a thickness of $T_{sub} = 0.25$ mm, a dielectric constant of 3.5 and a loss tangent of 0.0018.

Fig. 2 shows a closer look at the unit cell. It is comprised of two dipole antennas fed by an integrated balun structure similar to the broadside radiating 2D TCDA operating at

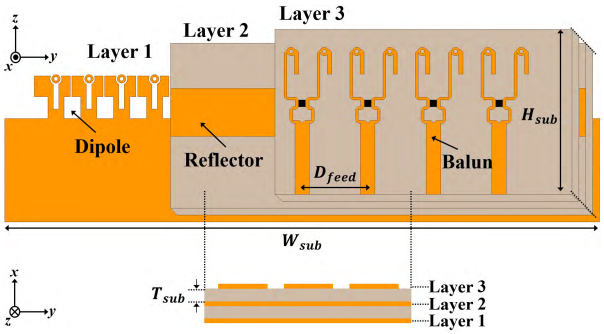

FIGURE 1. Geometry of the proposed TCDA antenna.

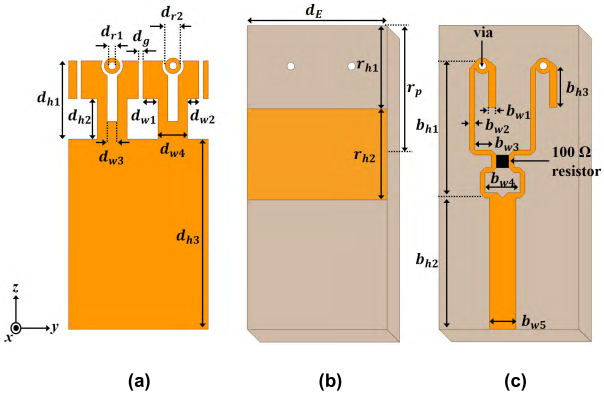

FIGURE 2. Geometry of the unit cell. (a) Layer 1: dipole; (b) Layer 2: reflector; and (c) Layer 3: excitation balun.

sub-6 GHz frequency bands [22], [23]. The square unit cells of conventional TCDA have an input impedance of 200 Ω, thus, baluns of such configuration include a 50 to 200 Ω impedance transformer, which would increase the weight and size of the antenna. To eliminate the need for the impedance transformer, Layer 1 in the proposed structure consists of two dipoles in a unit cell. Each of the two dipoles in the unit cell reduces the input impedance from 200 Ω to 100 Ω so that the balun can be implemented without an impedance transformer. As a result, the unit cell width was set at $d_E = 4.8$ mm ($0.5\ \lambda_{high}$) and two dipoles were placed at $d_g = 0.125$ mm intervals in the unit cell. In accordance with the Layer 1, Layer 3 has a one-to-two Wilkinson power divider that acts as a balun.

The Wilkinson power divider consists of a single 50 Ω input connected to the coaxial connector and two 100 Ω outputs connected to the dipoles. In addition, the output end of the balun has an open stub to compensate for incomplete impedance matching. The balun in Layer 3 was connected to Layer 1 through via to provide excitation at the feeding point of the dipole.

In order to implement TCDA in a fully planar form, the ground plane perpendicular to the antenna array should be removed. However, the removal of the vertical ground plane disperses the radiation pattern and lower the array gain, so to solve this problem, we placed the reflector at Layer 2.

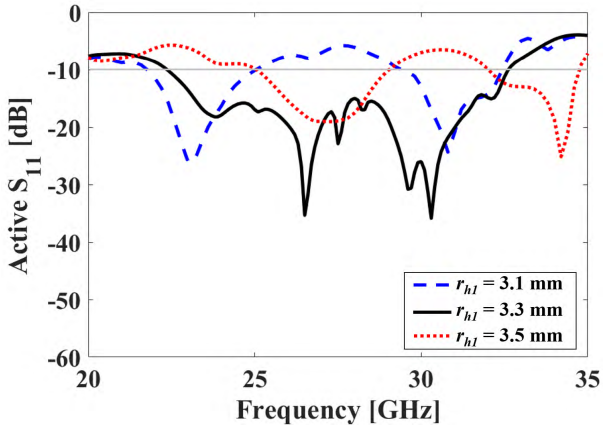

(a)

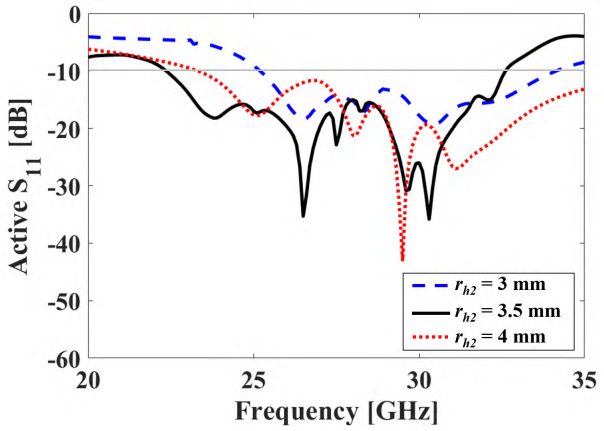

(b)

FIGURE 3. Active S_{11} of the TCDA by varying (a) the position of the reflector (r_{h1}); (b) height of the reflector (r_{h2}).

TABLE 2. Antenna parameters (UNITS : mm).

Parameters	Value	Parameters	Value	Parameters	Value
d_E	4.8	d_{w4}	1.18	b_{h2}	5.2
d_{h1}	3.1	d_{r1}	0.3	b_{h3}	1.6
d_{h2}	1.6	d_{r2}	0.6	b_{w1}	0.3
d_{h3}	7.54	d_g	0.125	b_{w2}	0.2
d_{w1}	0.645	r_{h1}	3.3	b_{w3}	0.66
d_{w2}	0.45	r_{h2}	3.5	b_{w4}	1.4
d_{w3}	0.4	b_{h1}	5.1	b_{w5}	1.05

Simulation results in the next sub-section show that inserting the reflector effectively concentrates the radiations to the desired direction ($\theta = 0°$).

B. EFFECT OF THE REFLECTOR

Fig. 3(a) and (b) show parametric studies on the effect on S_{11} due to the reflector's location (r_{h1}) and size (r_{h2}). All the other parameters were kept constant to the values in Table 2. Based on this, the optimized size and location parameters were found to be $r_{h1} = 3.3$ mm, $r_{h2} = 3.5$ mm, close to

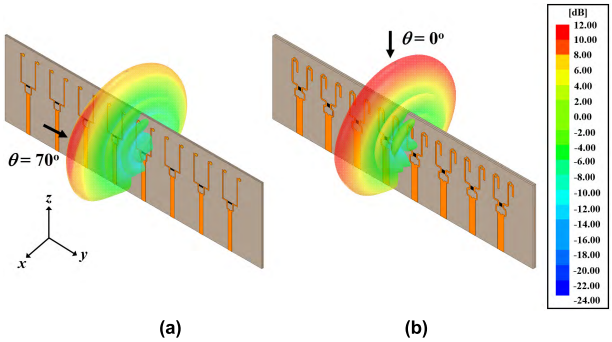

(a) (b)

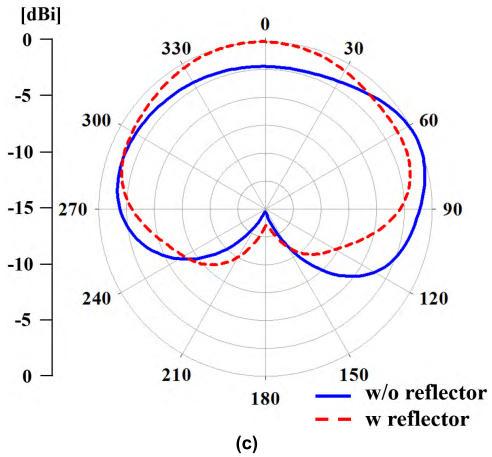

(c)

FIGURE 4. Comparison of the 3-D radiation patterns of 1 × 8 TCDA at 28 GHz: (a) without reflector; (b) with reflector; and (c) normalized 2D radiation pattern in *H*-plane (*x*-*z* plane).

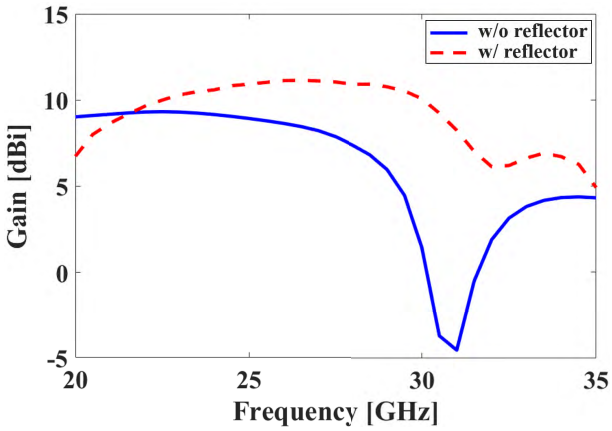

FIGURE 5. Comparison of the simulated antenna gain at $\theta = 0°$ between without and with the reflector surface.

$\lambda_{high}/2$ distance from the top of the dipole to the midpoint of the PEC reflector.

Fig. 4 shows the simulated 3D and 2D radiation patterns with and without the reflector. As can be seen in Fig. 4(a), the peak gain occurs at the x-axis ($\theta = 70°$) when the reflector is not placed. On the contrary, Fig. 4(b) with the reflector clearly demonstrates that the peak gain occurs at the desired direction ($\theta = 0°$) by concentrating the radiating components that leak in unwanted directions to the main lobe. Comparison of the $\theta = 0°$ gain with and without the reflector (Fig. 5) confirms

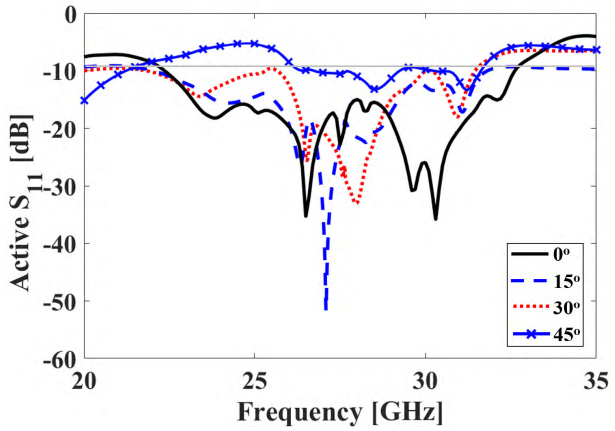

FIGURE 6. Simulated Active S_{11} in 0°., 15°, 30° and 45° scanning condition in *E*-plane (*y*-*z* plane) with the optimized 1 × 8 TCDA antenna.

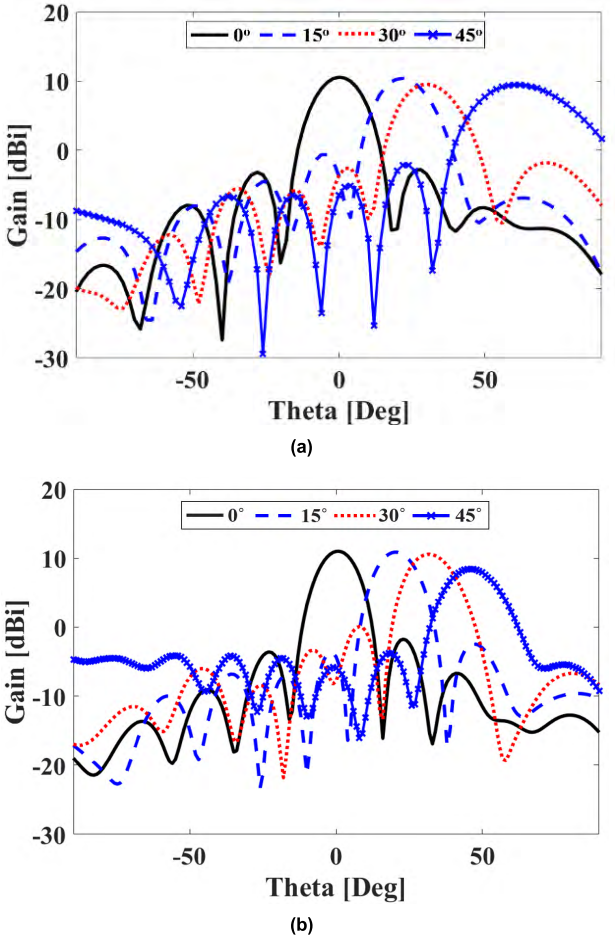

FIGURE 7. Simulated radiation pattern of 1 × 8 TCDA antenna at *E*-plane (*y*-*z* plane cut): (a) 24 GHz and (b) 28 GHz.

that the reflector improves the gain about 1 – 3.4 dBi in the frequency range interest, 23 – 30 GHz.

C. SIMULATION RESULTS FOR OPTIMIZED 1 X 8 TCDA ANTENNA

Fig. 6 shows the active S_{11} [24] according to the scanning angle in *E*-plane (*y*-*z* plane) of the optimized 1 × 8 TCDA antenna. For $\theta = 0°$, the proposed antenna showed that the active $S_{11} < -10$ dB bandwidth span from 22.6 to 32.5 GHz (Fractional bandwidth (FBW) = 36%). Full-wave simulation results showed that approximately 4:1 (12.8 – 51 GHz) impedance matching bandwidth was achievable for a TCDA when the ideal 100 Ω port was assigned at the excitation. After applying the balun, however, the bandwidth narrowed down to 1.44:1 (22.6 – 32.5 GHz) due to the bandwidth limitation of the GAMMA open-stubs [27].

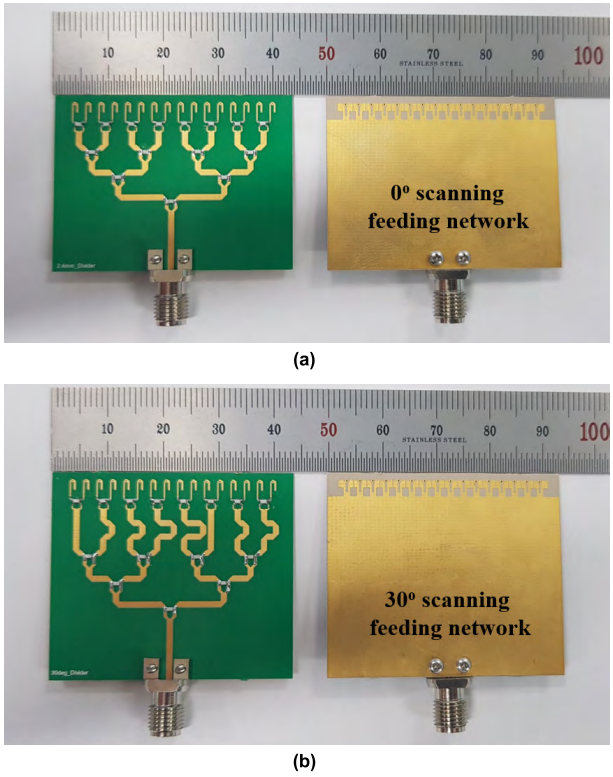

FIGURE 8. Photograph of the fabricated TCDA antenna with feeding network: (a) 0° scanning prototype and (b) 30° scanning prototype.

For $\theta = 30°$ scanning, the wideband performance was maintained over the range of 22.6 to 31 GHz (FBW = 32%). However, at $\theta = 45°$, the active $S_{11} < -10$ dB bandwidth was reduced down from 26 to 31 GHz (FBW = 17.5%). The reason for such significant deterioration may be due to the surface waves and their reflections at the array edges [25]. These surface waves intensify unwanted mutual coupling between array elements and degrade the scan impedance characteristic.

Fig. 7 shows the simulated *E*-plane radiation patterns of the optimized 1 × 8 TCDA. The detailed parameters of the optimized antenna are summarized in Table 2. As in Fig. 7(a), at 24 GHz, the antenna peak gain was 10.5 dBi and the Side Lobe Level (SLL) was −13 dBi at $\theta = 0°$. The similar patterns were observed for the 28 GHz patterns, Fig. 7(b), the peak gain was 11.2 dBi and the SLL was -13.5 dBi at $\theta = 0°$. The radiation patterns at different scanning angles were examined by varying the phase values at the antenna elements feeds. It was observed that preferable high gain

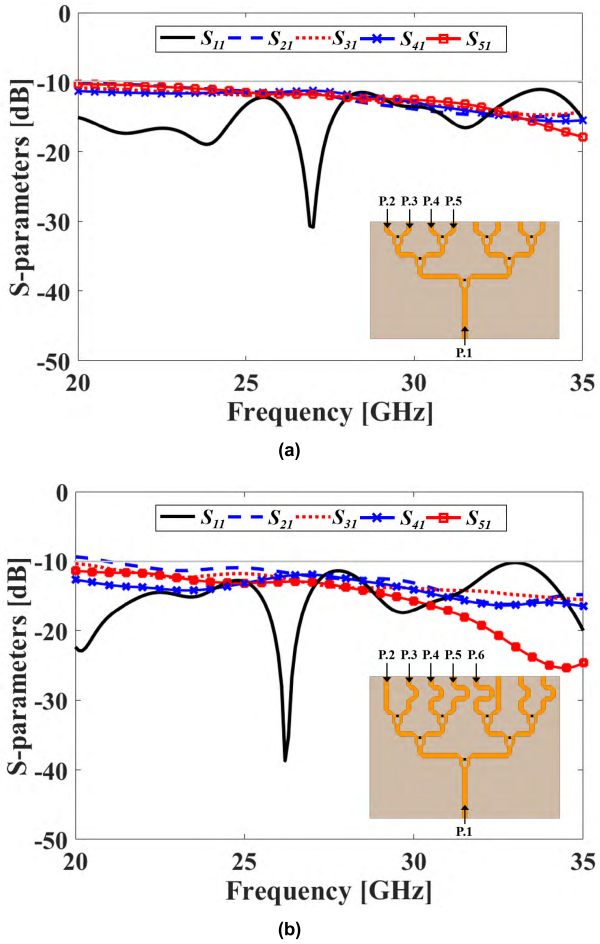

FIGURE 9. Simulated S–parameters of 8-way feeding network: (a) 0° scan feeding network (p.2, p.3, p.4, p.5 = 0°) and (b) 30° scan feeding network (p.2 = 0°, p.3 = −80°, p.4 = −160°, p.5 = −240°, p.6 = −320°).

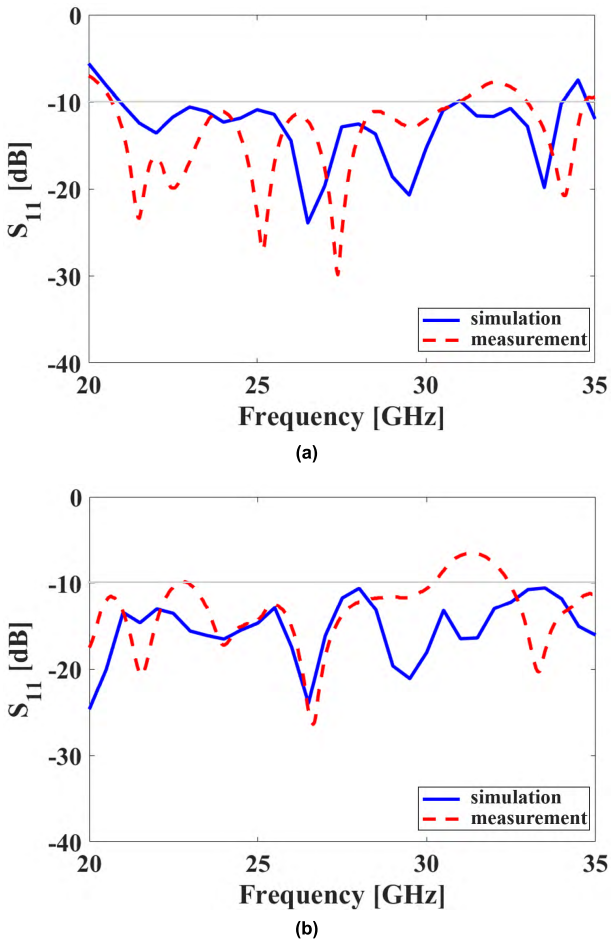

FIGURE 10. Simulated and measured S_{11} of the proposed TCDA antenna: (a) 0° scanning prototype and (b) 30° scanning prototype.

beam patterns could be maintained for scanning angle 15° and 30°. However, for $\theta = 45°$, undesirable beamwidth increase or gain drop were accompanied due to poor scanning impedance performance exhibited in Fig. 6 [19]. We note that the simulated radiation efficiencies were 96.36% (24 GHz), 97.48% (26 GHz), 97.06% (28 GHz), and 96.75% (30 GHz).

III. ANTENNA FABRICATION AND MEASUREMENT

A. FABRICATION OF TCDA PROTOTYPE

1 × 8 TCDA prototypes were fabricated using the multilayer PCB manufacturing technique. Two types of prototype were fabricated to verify scanning performance as shown in Fig. 8. They include 8-way feeding networks using the standard Wilkinson power divider for fixed different scanning angle. More specifically, Fig. 8(a) and (b) have the feeding networks that steer the beam to $\theta = 0°$ and $\theta = 30°$.

Prior to the fabrication, the Wilkinson divider's performances were examined using full-wave simulations. Fig. 9(a) shows the simulated S-parameters of the $\theta = 0°$ scan feeding network, which allowed for even power distribution performance with low reflection over a wide bandwidth. Meanwhile, Fig. 9(b) shows the simulated S-parameters of the $\theta = 30°$ scan feeding network. To achieve $\theta = 30°$ scanning, a length extension was applied to each transmission line to produce a phase delay of –80° between the output ports. The designed $\theta = 30°$ scanning feeding network also demonstrated wide bandwidth and good power distribution performance. Both feeding networks used a 100 Ω resistor to isolate each output port. Having verified by simulations, the feeding network output ports were connected to the baluns in the TCDA antenna array.

B. REFLECTION COEFFICIENT

The input ports of the 1 × 8 TCDA prototypes were connected to a HIROSE Electronics 2.92 mm coaxial connector. The reflection coefficient measurements of the fabricated prototypes were performed with an Anritsu Network Analyzer MS4644A.

Fig. 10 illustrate the simulated and measured impedance bandwidths of the fabricated TCDA antenna. For the 0° scanning measurement prototype, the simulated and measured contiguous bandwidths were 20.8 – 34 GHz (FBW = 48%), 20.5 – 31.5 GHz (FBW = 42%) within $S_{11} < -10$ dB,

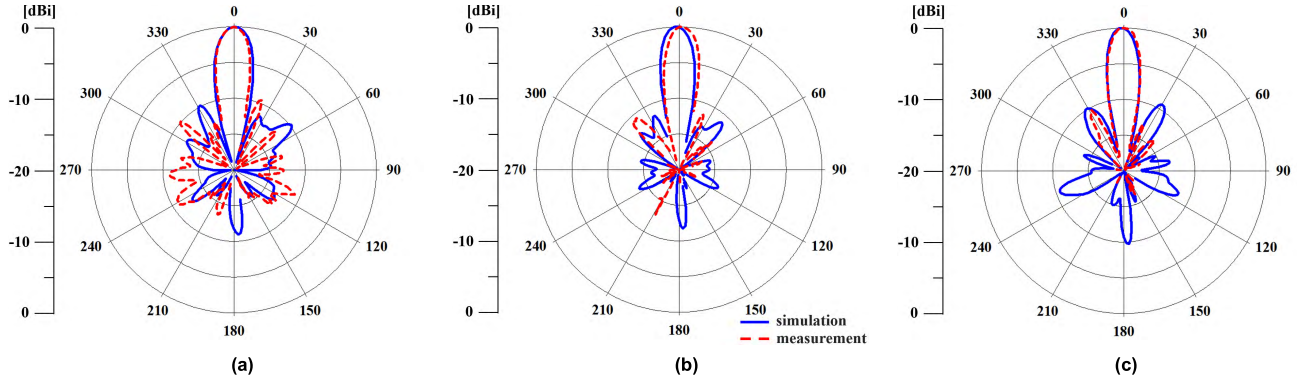

FIGURE 11. Simulated and measured radiation patterns of proposed TCDA antenna at a 0° beam scanning: (a) 24 GHz; (b) 26 GHz; and (c) 28 GHz.

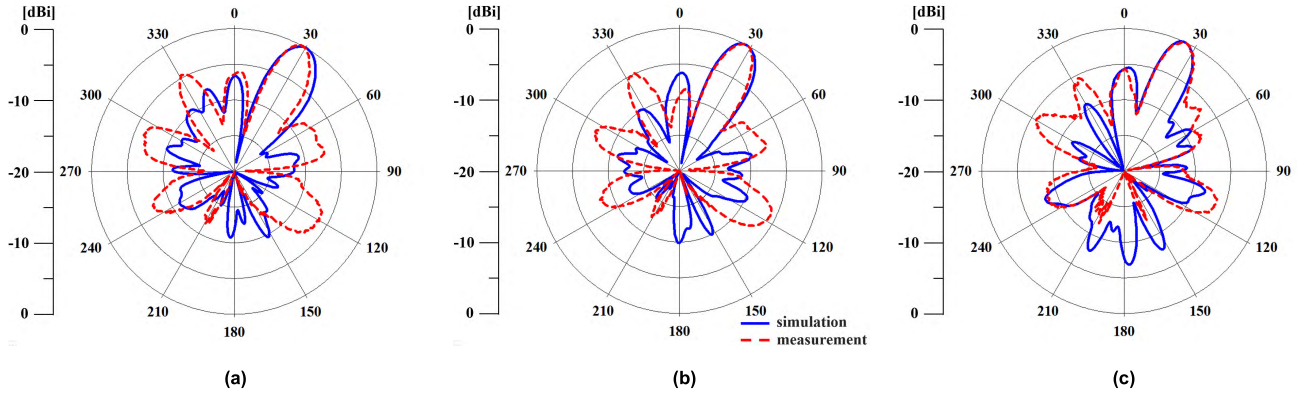

FIGURE 12. Simulated and measured radiation patterns of proposed TCDA antenna at a 30° beam scanning: (a) 24 GHz; (b) 26 GHz; and (c) 28 GHz.

respectively. On the other hand, for the $\theta = 30°$ scanning measurement prototype, the simulated and measured bandwidth were 20 - 35 GHz (FBW = 54%) and 20 - 31 GHz (FBW = 43%) within $S_{11} < -10$ dB, respectively. The measurement results of the two prototypes showed good agreement and wideband characteristics, except that S_{11} was higher than –10 dB at the 31 to 33 GHz band, which was unlike the simulated results. This discrepancy was due to the fabrication error. The 3-layered antenna was constructed by putting two separately fabricated PCBs together using adhesive. The volume of the adhesive has expanded after solidified, resulting in irregular thickness of the fabricated array. This affected not only the S_{11} but also the antenna gain and side-lobe level.

C. RADIATION PATTERN

Fig. 11 and Fig. 12 depict the simulated and measured radiation patterns of the proposed TCDA antenna in the E-plane (y-z plane cut). Fig. 11 presents the normalized radiation pattern of the $\theta = 0°$ prototype. The measured radiation pattern was validated along with the simulated results. The TCDA antenna achieved gains of 5.3, 6.1, and 5.2 dBi at 24, 26, and 28 GHz, respectively, which were less than the simulated peak gains of 7.7, 8.9, and 7.6 dBi respectively. Nevertheless, as shown in Fig. 12 for all of the representative frequencies,

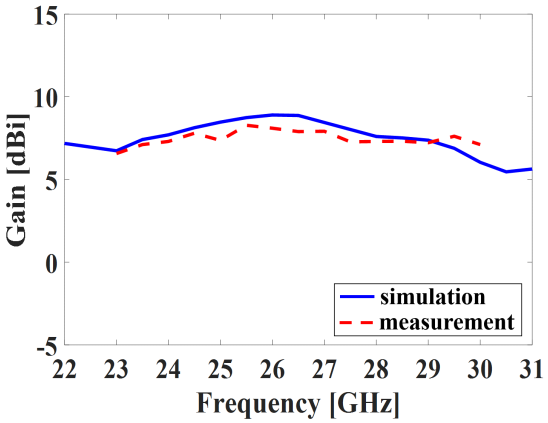

FIGURE 13. Simulated and measured gain of the fabricated 0° scanning prototype.

it can be seen that SLL < -10 dBi and the Half Power Beam Width (HPBW) $< 14.7°$ and good agreement with the simulated results.

Fig. 12 presents the normalized radiation pattern of the $\theta = 30°$ scanning measurement prototype. The TCDA antenna achieved gains of 5.4, 6.2, 5.1 dBi at 24, 26, and 28 GHz, respectively, which were less than the simulated peak gains

of 6.3, 7.6, and 6.2 dBi, respectively. Also, the measured results showed larger side lobes than the simulation results. This may be due to the abrupt transitions of the Wilkinson divider branches in the proximity of PCB edges as seen Fig. 8(b). Unwanted radiation may occur from here and possibly be induced to the straight line next to it. Also, the thickness change due to the adhesive may affect the side-lobe level. Nevertheless, it was confirmed that the main lobe of the antenna formed a fan beam at $\theta = 30°$. Based on these analyses, we believe that better measurement result would be obtained if a sophisticated feeding network or phase shifter is applied to the proposed TCDA antenna.

Fig. 13 shows the measured and simulated gains for the 0° scanning prototype. We note that the measured data was compensated with a cable loss of 2.5 dB in the frequency of interest.

IV. CONCLUSION

A 1D TCDA antenna that can cover both 5G mmWave candidate bands in the range 23 - 30 GHz was described and proposed. The unit cell was comprised of two tightly coupled dipoles and the Gamma shaped balun as a feed. Based on the unit cell, 1×8 TCDA prototypes were designed, optimized, fabricated and tested to prove their capability of wideband characteristics. Different from the previous TCDAs, the proposed design substituted the vertical ground to a horizontal reflector layer compatible with the multilayer PCB fabrication process. In this context, the proposed TCDA was able to maintain desirable radiation characteristics and ultra low profile structure applicable in a small area of a mobile handset.

According to comparisons between the simulated and measured results of the proposed TCDA antenna, we demonstrated wideband characteristic covering all the target frequency bands. The FBW based on $S_{11} < -10$ dB is 36% (22.6 – 32.5 GHz) which is more than two times as broad as 14.6% (24.6 – 28.5 GHz) reported for a Vivaldi array [28].

However, the gain, SLL and scanning beam of the fabricated prototype were degraded from the simulation results due to the surface waves in the finite footprint. The surface waves can be mitigated by placing a superstrate parallel to the array [26] or employing resistive elements at the array edges [25]. Based on these considerations, further research is underway to carry out an improved prototype.

REFERENCES

[1] *Framework and Overall Objectives of the Future Development of IMT for 2020 and Beyond*, document ITU-R M.2083-0, International Telecommunication Union-Radiocommunication Sector, Geneva, Switzerland, Sep. 2015.
[2] T. S. Rappaport *et al.*, "Millimeter wave mobile communications for 5G cellular: It will work!" *IEEE Access*, vol. 1, pp. 335–349, May 2013.
[3] M. J. Marcus, "WRC-19 issues: A survey," *IEEE Wireless Commun.*, vol. 24, no. 1, pp. 2–3, Feb. 2017.
[4] "5G spectrum recommendations," 5G Americas, White Paper, Apr. 2017.
[5] M. Asaadi and A. Sebak, "High-gain low-profile circularly polarized slotted SIW cavity antenna for MMW applications," *IEEE Antennas Wireless Propag. Lett.*, vol. 16, pp. 752–755, Aug. 2017.
[6] Y. Cao, K.-S. Chin, W. Che, W. Yang, and E. S. Li, "A compact 38 GHz multibeam antenna array with multifolded butler matrix for 5G applications," *IEEE Antennas Wireless Propag. Lett.*, vol. 16, pp. 2996–2999, 2017.
[7] N. Yoon and C. Seo, "A 28-GHz wideband 2×2 U-slot patch array antenna," *J. Electromagn. Eng. Sci.*, vol. 17, no. 3, pp. 133–137, Jul. 2017.
[8] S. F. Jilani and A. Alomainy, "A multiband millimeter-wave 2-D array based on enhanced franklin antenna for 5G wireless systems," *IEEE Antennas Wireless Propag. Lett.*, vol. 16, pp. 2983–2986, Sep. 2017.
[9] C. X. Mao, S. Gao, and Y. Wang, "Broadband high-gain beam-scanning antenna array for millimeter-wave applications," *IEEE Trans. Antennas Propag.*, vol. 65, no. 9, pp. 4864–4868, Jul. 2017.
[10] W. Hong, K.-H. Baek, Y. Lee, Y. Kim, and S.-T. Ko, "Study and prototyping of practically large-scale mmWave antenna systems for 5G cellular devices," *IEEE Commun. Mag.*, vol. 52, no. 9, pp. 63–69, Sep. 2014.
[11] W. Hong, S.-T. Ko, Y. Lee, and K.-H. Baek, "Compact 28 GHz antenna array with full polarization flexibility under yaw, pitch, roll motions," in *Proc. 9th Eur. Conf. Antennas Propag. (EuCAP)*, Lisbon, Portugal, Apr. 2015, pp. 1–3.
[12] B. Yu, K. Yang, C.-Y.-D. Sim, and G. Yang, "A novel 28 GHz beam steering array for 5G mobile device with metallic casing application," *IEEE Trans. Antennas Propag.*, vol. 66, no. 1, pp. 462–466, Jan. 2018.
[13] S.-J. Park, D.-H. Shin, and S.-O. Park, "Low side-lobe substrate-integrated-waveguide antenna array using broadband unequal feeding network for millimeter-wave handset device," *IEEE Trans. Antennas Propag.*, vol. 64, no. 3, pp. 923–932, Mar. 2016.
[14] S. X. Ta, H. Choo, and I. Park, "Broadband printed-dipole antenna and its arrays for 5G applications," *IEEE Antennas Wireless Propag. Lett.*, vol. 16, pp. 2183–2186, May 2017.
[15] S. Ershadi, A. Keshtkar, A. H. Abdelrahman, and H. Xin, "Wideband high gain antenna subarray for 5G applications," *Prog. Electromagn. Res.*, vol. 78, pp. 33–46, 2017.
[16] B. A. Munk, *Finite Antenna Arrays and FSS*, 1st ed. New York, NY, USA: Wiley, 2003.
[17] J. P. Doane, K. Sertel, and J. L. Volakis, "A wideband, wide scanning tightly coupled dipole array with integrated balun (TCDA-IB)," *IEEE Trans. Antennas Propag.*, vol. 61, no. 9, pp. 4538–4548, Sep. 2013.
[18] W. F. Moulder, K. Sertel, and J. L. Volakis, "Ultrawideband superstrate-enhanced substrate-loaded array with integrated feed," *IEEE Trans. Antennas Propag.*, vol. 61, no. 11, pp. 5802–5807, Nov. 2013.
[19] E. Yetisir, N. Chalichechian, and J. L. Volakis, "Ultrawideband array with 70° scanning using FSS superstrate," *IEEE Trans. Antennas Propag.*, vol. 64, no. 10, pp. 4256–4265, Oct. 2016.
[20] H. Zhang, S. Yang, Y. Chen, J. Guo, and Z. Nie, "Wideband dual-polarized linear array of tightly coupled elements," *IEEE Trans. Antennas Propag.*, vol. 66, no. 1, pp. 476–480, Jan. 2018.
[21] H. Lee and S. Nam, "A dual-polarized 1-D tightly coupled dipole array antenna," *IEEE Trans. Antennas Propag.*, vol. 65, no. 9, pp. 4511–4518, Sep. 2017.
[22] J. P. Doane, K. Sertel, and J. L. Volakis, "A 6.3:1 bandwidth scanning tightly coupled dipole array with co-designed compact balun," in *Proc. IEEE Int. Symp. Antennas Propag. (APSURSI)*, Jul. 2012, pp. 1–2.
[23] D. Cavallo, A. Neto, and G. Gerini, "PCB slot based transformers to avoid common-mode resonances in connected arrays of dipoles," *IEEE Trans. Antennas Propag.*, vol. 58, no. 8, pp. 2767–2771, Aug. 2010.
[24] W. Kahn, "Active reflection coefficient and element efficiency in arbitrary antenna arrays," *IEEE Trans. Antennas Propag.*, vol. AP-17, no. 5, pp. 653–654, Sep. 1969.
[25] B. A. Munk, D. S. Janning, J. B. Pryor, and R. J. Marhefka, "Scattering from surface waves on finite FSS," *IEEE Trans. Antennas Propag.*, vol. 49, no. 12, pp. 1782–1793, Dec. 2001.
[26] E. Magill and H. A. Wheeler, "Wide-angle impedance matching of a planar array antenna by a dielectric sheet," *IEEE Trans. Antennas Propag.*, vol. AP-14, no. 1, pp. 49–53, Jan. 1966.
[27] J. A. Kasemodel, C.-C. Chen, and J. L. Volakis, "Wideband planar array with integrated feed and matching network for wide-angle scanning," *IEEE Trans. Antennas Propag.*, vol. 61, no. 9, pp. 4528–4537, Sep. 2013.
[28] S. Zhu, H. Liu, Z. Chen, and P. Wen, "A compact gain-enhanced Vivaldi antenna array with suppressed mutual coupling for 5G mmWave application," *IEEE Antennas Wireless Propag. Lett.*, vol. 17, no. 5, pp. 776–779, May 2018.

JAE-YEON SHIM received the B.S. degree in electrical and information engineering from the Seoul National University of Science and Technology, Seoul, South Korea, in 2017, where he is currently pursuing the M.S. degree. His research interests include electrically small antenna a and millimeter-wave array antenna design.

JONG-GYU GO received the M.S. degree in electrical and information engineering from the Seoul National University of Science and Technology, Seoul, South Korea, in 2017. His current research interests include electrically small antenna a and RF and microwave circuit design.

JAE-YOUNG CHUNG received the B.S. degree from Yonsei University, South Korea, in 2002, and the M.S. and Ph.D. degrees from The Ohio State University, USA, in 2007 and 2010, respectively, all in electrical engineering. From 2002 to 2004, he was with Motorola, South Korea, as an RF Engineer. From 2010 to 2012, he was with Samsung Electronics, South Korea, as an Antenna Engineer. He is currently an Associate Professor with the Department of Electrical and Information Engineering, Seoul National University of Science and Technology, South Korea. His research interests include electromagnetic measurement and antenna design.